21

Kinematics, Singularity and Dexterity Analysis of Planar Parallel Manipulators Based on DH Method

Serdar Kucuk
Kocaeli University
Turkey

1. Introduction

Parallel manipulators have separate serial kinematic chains that are linked to the ground and the moving platform at the same time. They have some potential advantages over serial robot manipulators such as high accuracy, greater load capacity, high mechanical rigidity, high velocity and acceleration (Kang et al., 2001; Kang & Mills, 2001). Planar Parallel Manipulators (PPMs), performing two translations along the x and y axes, and rotation through an angle of ϕ around the z axis are a special group among the parallel robot manipulators. They have potential advantages for microminiaturization (Hubbard et al., 2001) and pick-and-place operations (Heerah et al., 2003). However, due to the complexity of the closed-loop chain mechanism, the kinematics analysis of parallel manipulators is more difficult than their serial counterparts. Therefore selection of an efficient mathematical model is very important for simplifying the complexity of the kinematics problems in parallel robots. In this book chapter, the forward and inverse kinematics problems of PPMs are solved based on D-H method (Denavit & Hartenberg, 1955) which is a common kinematic modelling convention using 4x4 homogenous transformation matrices. The easy physical interpretation of the robot mechanisms is the main advantage of this method. The Forward kinematics problem calculates the position and orientation of the end-effector if the set of joint angles are known. The inverse kinematics problem solves for the joint angles when the position and orientation of the end effector is given. In contrast to serial manipulators, the forward kinematics problem is much more difficult than the inverse kinematic problem for parallel manipulators. Afterwards very practical definitions are provided for Jacobian matrix and workspace determination of PPMs which are required for singularity and dexterity analyses. Rest of this book chapter is composed of the following sections. Some fundamental definitions about D-H method as a kinematics modelling convention, Jacobian matrix, condition number, global dexterity index, singularity and workspace determination are presented in Section 2. A two-degree-of-freedom (2-dof) PPM and a 3-dof Fully Planar Parallel Manipulator (FPPM) are given as examples to illustrate the methodology in the following Section. FPPMs are composed of a moving platform linked to

the ground by three independent limbs including one active (actuated) joint in each (Merlet, 1996). The conclusions with final remarks are presented in the last section.

2. Background

2.1 Denavit-Hartenberg convention

The D-H convention (Denavit & Hartenberg, 1955) based on 4x4 homogenous transformation matrices is commonly used kinematic modelling convention for the robotics community. The easy physical interpretation of the robot mechanisms is the main advantage of this method. A spatial transformation between two consecutive links can be described by a set of parameters, namely α_{j-1}, a_{j-1}, θ_j and d_j. Using these parameters, the general form of the transformation matrix for adjacent coordinate frames, j-1 and j is obtained as

$$ {}^{j-1}_{j}T = \begin{bmatrix} \cos\theta_j & -\sin\theta_j & 0 & a_{j-1} \\ \sin\theta_j \cos\alpha_{j-1} & \cos\theta_j \cos\alpha_{j-1} & -\sin\alpha_{j-1} & -\sin\alpha_{j-1} d_j \\ \sin\theta_j \sin\alpha_{j-1} & \cos\theta_j \sin\alpha_{j-1} & \cos\alpha_{j-1} & \cos\alpha_{j-1} d_j \\ 0 & 0 & 0 & 1 \end{bmatrix} \tag{1} $$

The transformation of the link n coordinate frame into the base coordinate frame of the robot manipulator is given by

$$ {}^{j-1}_{n}T = {}^{j-1}_{j}T \; {}^{j}_{j+1}T \, {}^{j+1}_{j+2}T \cdots {}^{n-1}_{n}T \tag{2} $$

where j=1, 2, 3, ..., n.

2.2 Jacobian Matrix, Condition Number and Global Dexterity Index

Dexterity is an essential topic for design and conceptual control of robotic manipulators. It can be described as the ability to perform infinitesimal movement in the arbitrary directions as easily as possible in the workspace of the robotic manipulators. It is based on the condition number (κ) of the manipulator Jacobian matrix (Gosselin & Angeles, 1991).

$$ \kappa = \|J\| \left\| J^{-1} \right\| \tag{3} $$

where J illustrates the Jacobian matrix and $\| \cdot \|$ denotes the Frobenius norm of the matrix. κ varies between 1 to ∞. In general, $\eta = 1/\kappa$ is used for limiting the dexterity between 0 and 1. Thus dexterity of a manipulator can be easily measured. It is well known that as $\eta=1$ represents a perfect isotropic dexterity, $\eta=0$ illustrates singular configuration. Then the kinematic relations for the planar parallel manipulators can be expressed as

$$ f(\mathbf{x},\mathbf{q})=0 \tag{4} $$

where f is the function of $\mathbf{x}=(x,y,\phi)^T$ and $\mathbf{q}=(q_1, q_2, \text{and } q_n)^T$, and 0 is n dimensional zero vector. The parameters x, y and ϕ are the position and orientation of the end-effector in terms of base frame. Additionally, q_1, q_2 and q_n represent the actuated joint variables. The following term is obtained differentiating the equation 4 with respect to the time.

$$A\dot{\mathbf{x}}+B\dot{\mathbf{q}}=0 \tag{5}$$

where $\dot{\mathbf{x}}$ and $\dot{\mathbf{q}}$ are the time derivatives of $\mathbf{x}$ and $\mathbf{q}$, respectively. A and B are two separate Jacobian matrices. The overall Jacobian matrix for a parallel manipulator can be obtained as

$$J=-B^{-1}A \tag{6}$$

Since the dexterity demonstrates the local property of a mechanism, designers requires a global one. Gosselin and Angeles (1991) introduced Global Dexterity Index (GDI) in order to measure the global property of the manipulators. GDI defined as

$$GDI=\frac{A}{B} \tag{7}$$

where B represents the area of the workspace and A is

$$A=\int_{\phi}\int_{y}\int_{x}\left(\frac{1}{\kappa}\right)dxdyd\phi \tag{8}$$

2.3 Singularity

Three types of singularities exist for planar parallel manipulators (Tsai, 1999; Merlet, 2000). They occur when either determinant of the matrices A or B or both are zero. When the determinant of A and B goes to zero, the direct and inverse kinematics singularities occur, respectively. Direct kinematics singularity occurs inside the workspace of the manipulator. Inverse kinematics singularity occurs at the boundaries of the manipulator's workspace where any limb is completely stretched-out or folded-back.

2.4 Workspace Determination

Workspace determination is a very significant step in analyzing robot manipulators. Its determination is necessary for conceptual design and trajectory planning. Many researches (Agrawal, 1990; Gosselin, 1990; Merlet, 1995; Merlet et al., 1998) focused on the workspace determination of parallel manipulators. Merlet, Gosselin and Mouly (1998) outlined some workspace definitions for PPMs such as constant orientation workspace, reachable workspace and dexterous workspace. The constant orientation workspace (considered also in this book chapter) is the area that can be reached by the end-effector with constant orientation. In general, geometrical (Bonev & Ryu, 2001; Gosselin & Guillot, 1991) and numerical methods (Kim et al., 1997) are used for workspace determination of parallel manipulators. Computation of workspace based on geometrical method is difficult and may not be obtained due to the complexity of the closed-loop chain mechanisms (Fichter, 1986).

Alternatively, numerical methods based on the discretization of Cartesian space (Kim et al., 1997) in general, are also used in this study due to their simplicity according to the geometrical methods. In discretization method, firstly a Cartesian area is discretized into "PxQ" points along the X and Y axes. Secondly each pose in this discretized Cartesian area is examined whether belonging to the workspace of the manipulator.

3. Examples

3.1. The 2-dof RPR planar parallel manipulator

The 2-dof RPR (Revolute-Prismatic-Revolute) planar parallel manipulator given by Figure 1 has two limbs B_iM_i, where i=1, 2, a moving platform M_1M_2 and a fixed base B_1B_2. The lengths of the actuated prismatic joints vary between $d_{i(min)}$ and $d_{i(max)}$. The end-effector is attached to the pint P on the moving platform. The position $P(p_x, p_y)$ and orientation (ϕ) of the end-effector is defined with respect to the {XYZ} coordinate system.

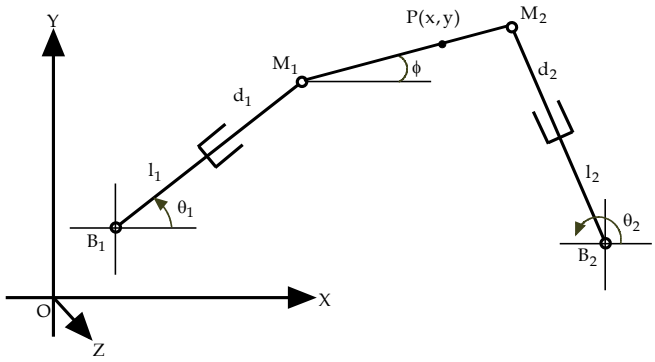

Fig. 1. The planar 2-dof RPR parallel manipulator.

The following equation can be written using the geometric identities on Figure 1.

$$OB_i + B_iM_i = OP + PM_i \tag{9}$$

where i=1, 2.

In order to solve **the inverse kinematics problem**, the relation in equation 9 is adapted to the manipulator in Figure 1. Thus the ${}^{M_i}_{O_i}T^1$ and ${}^{M_i}_{O_i}T^2$ homogeneous transformation matrices can be obtained as

$$
\begin{aligned}
{}^{M_i}_{O_i}T^1 &= \begin{bmatrix} 1 & 0 & 0 & OB_{x_i} \\ 0 & 1 & 0 & OB_{y_i} \\ 0 & 0 & 1 & 0 \\ 0 & 0 & 0 & 1 \end{bmatrix} \begin{bmatrix} \cos\theta_i & -\sin\theta_i & 0 & 0 \\ \sin\theta_i & \cos\theta_i & 0 & 0 \\ 0 & 0 & 1 & 0 \\ 0 & 0 & 0 & 1 \end{bmatrix} \begin{bmatrix} 1 & 0 & 0 & 0 \\ 0 & 0 & 1 & l_i + d_i \\ 0 & -1 & 0 & 0 \\ 0 & 0 & 0 & 1 \end{bmatrix} \\
&= \begin{bmatrix} \cos\theta_i & 0 & \sin\theta_i & OB_{x_i} - \sin\theta_i(d_i + l_i) \\ \sin\theta_i & 0 & -\cos\theta_i & OB_{y_i} + \cos\theta_i(d_i + l_i) \\ 0 & 1 & 0 & 0 \\ 0 & 0 & 0 & 1 \end{bmatrix}
\end{aligned} \tag{10}
$$

$$
\begin{aligned}
{}^{M_i}_{O_i}T^2 &= \begin{bmatrix} 1 & 0 & 0 & p_x \\ 0 & 1 & 0 & p_y \\ 0 & 0 & 1 & 0 \\ 0 & 0 & 0 & 1 \end{bmatrix} \begin{bmatrix} \cos\gamma_i & -\sin\gamma_i & 0 & 0 \\ \sin\gamma_i & \cos\gamma_i & 0 & 0 \\ 0 & 0 & 1 & 0 \\ 0 & 0 & 0 & 1 \end{bmatrix} \begin{bmatrix} 1 & 0 & 0 & PM_i \\ 0 & 1 & 0 & 0 \\ 0 & 0 & 1 & 0 \\ 0 & 0 & 0 & 1 \end{bmatrix} \\
&= \begin{bmatrix} -\cos\phi & \sin\phi & 0 & p_x + PM_i\cos\gamma_i \\ -\sin\phi & -\cos\phi & 0 & p_y + PM_i\sin\gamma_i \\ 0 & 0 & 1 & 0 \\ 0 & 0 & 0 & 1 \end{bmatrix}
\end{aligned} \tag{11}
$$

where $\gamma_1 = \pi + \phi$ and $\gamma_2 = \phi$. Since the position vectors of ${}^{M_i}_{O_i}T^1$ and ${}^{M_i}_{O_i}T^2$ matrices are equal, one can write the following equations easily.

$$
\begin{bmatrix} -\sin\theta_i(d_i + l_i) \\ \cos\theta_i(d_i + l_i) \end{bmatrix} = \begin{bmatrix} p_x + PM_i\cos\gamma_i - OB_{x_i} \\ p_y + PM_i\sin\gamma_i - OB_{y_i} \end{bmatrix} \tag{12}
$$

Summing the squares of the both sides in the equation 12, we obtain, after simplification,

$$
\begin{aligned}
Q_i = {} & PM_i^2 + p_x^2 + p_y^2 + OB_{x_i}^2 + OB_{y_i}^2 - 2p_xOB_{x_i} - 2p_yOB_{y_i} \\
& + 2\cos\gamma_i PM_i(p_x - OB_{x_i}) + 2\sin\gamma_i PM_i(p_y - OB_{y_i}) - (d_i + l_i)^2 = 0
\end{aligned} \tag{13}
$$

The active joint variables d_i can be found using equation 13 as follows.

$$
d_i = \sqrt{\begin{aligned} & PM_i^2 + p_x^2 + p_y^2 + OB_{x_1}^2 + OB_{y_1}^2 - 2p_xOB_{x_i} - 2p_yOB_{y_i} \\ & + 2\cos\gamma_i PM_i(p_x - OB_{x_i}) + 2\sin\gamma_i PM_i(p_y - OB_{y_i}) \end{aligned}} - l_i \tag{14}
$$

Once the active joint variables d_1 and d_2 are solved, the passive joint variable θ_1 and θ_2 can be found from the equation 12 by back substitution.

$$\theta_i = a\tan 2\left(\frac{-p_x - PM_i\cos\gamma_i + OB_{x_i}}{(d_i + l_i)}, \frac{p_y + PM_i\sin\gamma_i - OB_{y_i}}{(d_i + l_i)}\right) \tag{15}$$

The Jacobian matrix of the 2-dof RPR is computed using the equation 13 as follows.

$$A\dot{x} + B\dot{q} = 0$$

$$\begin{bmatrix} \frac{\partial Q_1}{\partial p_x} & \frac{\partial Q_1}{\partial p_y} \\ \frac{\partial Q_2}{\partial p_x} & \frac{\partial Q_2}{\partial p_y} \end{bmatrix} \begin{bmatrix} \dot{p}_x \\ \dot{p}_y \end{bmatrix} + \begin{bmatrix} \frac{\partial Q_1}{\partial d_1} & \frac{\partial Q_1}{\partial d_2} \\ \frac{\partial Q_2}{\partial d_1} & \frac{\partial Q_2}{\partial d_2} \end{bmatrix} \begin{bmatrix} \dot{d}_1 \\ \dot{d}_2 \end{bmatrix} = 0$$

$$\begin{bmatrix} p_x - OB_{x_1} + \cos\gamma_1 PM_1 & p_y - OB_{y_1} + \sin\gamma_1 PM_1 \\ p_x - OB_{x_2} + \cos\gamma_2 PM_2 & p_y - OB_{y_2} + \sin\gamma_2 PM_2 \end{bmatrix} \begin{bmatrix} \dot{p}_x \\ \dot{p}_y \end{bmatrix} + \begin{bmatrix} -d_1 - l_1 & 0 \\ 0 & -d_2 - l_2 \end{bmatrix} \begin{bmatrix} \dot{d}_1 \\ \dot{d}_2 \end{bmatrix} = 0 \tag{16}$$

The overall Jacobian matrix is obtained as

$$J = \begin{bmatrix} -\frac{p_x - OB_{x_1} + \cos\gamma_1 PM_1}{-d_1 - l_1} & -\frac{p_y - OB_{y_1} + \sin\gamma_1 PM_1}{-d_1 - l_1} \\ -\frac{p_x - OB_{x_2} + \cos\gamma_2 PM_2}{-d_2 - l_2} & -\frac{p_y - OB_{y_2} + \sin\gamma_2 PM_2}{-d_2 - l_2} \end{bmatrix} \tag{17}$$

***Numerical example for the inverse kinematics*:** The dimensions of the planar 2-dof RPR parallel manipulator are given as $l_1=l_2=12$, $PM_1=PM_2=3$, $OB_{x1}=0$, $OB_{y1}=0$, $OB_{x2}=15$, $OB_{y2}=0$, $p_x=11$, $p_y=20$ and $\phi=30^o$. According to the data above, the active joint variables d_1 and d_2 can be found as 8.3185 and 9.5457, respectively. The passive joint variables θ_1 and θ_2 are found as -24.4256 and 3.7307, respectively by back substitution.

Numerical example for the Jacobian matrix and condition number: Using the dimensions of the inverse kinematics example above, the Jacobian matrix and condition number are found as

$$J = \begin{bmatrix} 0.4135 & 0.9105 \\ -0.0651 & 0.9979 \end{bmatrix} \text{ and } \kappa = 2.1192 \tag{18}$$

Numerical example for the workspace determination: The dimensions of the manipulator are given as $l_1=l_2=10$, $PM_1=PM_2=2$, $OB_{x1}=0$, $OB_{y1}=0$, $OB_{x2}=20$ and $OB_{y2}=0$ and. The lengths of the actuated prismatic joints vary between $d_i(min)=0$ and $d_i(max)=7$, where i=1,2. The workspace is obtained as 102.3888 for $\phi=0^o$ orientation. The limits of the discretized Cartesian area are denoted by the red rectangle shown in Figure 2a. The black and green areas show reachable and non-reachable workspaces of the manipulator, respectively.

Numerical example for the dexterity and singularity analysis: The Figure 2b shows the inverse dexterity of the manipulator using the same dimensions given by example for workspace determination. The GDI of the manipulator are found as 0.0012. As seen in Figure 2b, since the inverse of the condition numbers colored with red areas are so close to

the unity, there isn't any singular point occurred inside reachable workspace. The red and blue areas show reachable and non-reachable workspaces of the manipulator, respectively.

3.2. The 3-dof RPR planar parallel manipulator

The 3-dof RPR planar parallel manipulator shown in Figure 3 has three limbs B_iM_i, where i=1, 2, 3. P denotes the point where the end-effector is located at the moving platform which is chosen as equilateral triangle. The angle ϕ represents the orientation of the end-effector. If a line AB passing through the point *P* is drawn parallel to the M_1M_2, the angles PM_1M_2 (σ_1) and PM_2M_1 (σ_2) are equal to the angles APM_1 and M_2PB, respectively. The angles between the lines BP and PM_1, M_2P and PB, BP and PM_3 are denoted as λ_1, λ_2 and λ_3, respectively.

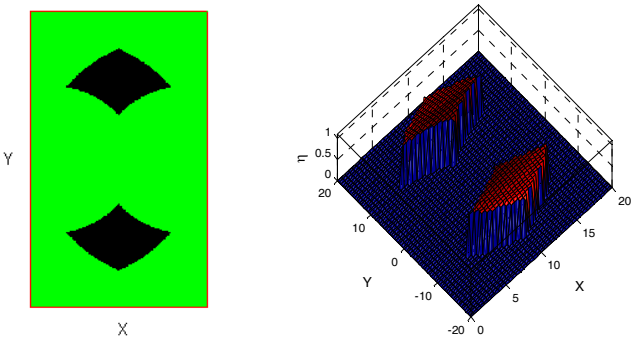

Fig. 2. a) Workspace, b) dexterity graph, for planar 2-dof RPR parallel manipulator.

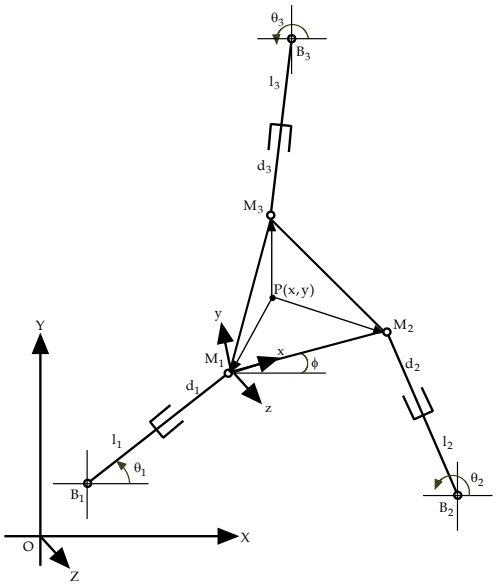

Fig. 3. The planar 3-dof RPR parallel manipulator.

If the relation in equation 9 is adapted to the manipulator in Figure 3, the ${}^{M_i}_{O_i}T^1$ and ${}^{M_i}_{O_i}T^2$ homogeneous transformation matrices can be obtained as

$$
\begin{aligned}
{}^{M_i}_{O_i}T^1 &= \begin{bmatrix} 1 & 0 & 0 & OB_{x_i} \\ 0 & 1 & 0 & OB_{y_i} \\ 0 & 0 & 1 & 0 \\ 0 & 0 & 0 & 1 \end{bmatrix} \begin{bmatrix} \cos\theta_i & -\sin\theta_i & 0 & 0 \\ \sin\theta_i & \cos\theta_i & 0 & 0 \\ 0 & 0 & 1 & 0 \\ 0 & 0 & 0 & 1 \end{bmatrix} \begin{bmatrix} 1 & 0 & 0 & 0 \\ 0 & 0 & 1 & l_i + d_i \\ 0 & -1 & 0 & 0 \\ 0 & 0 & 0 & 1 \end{bmatrix} \\
&= \begin{bmatrix} \cos\theta_i & 0 & \sin\theta_i & OB_{x_i} - \sin\theta_i (d_i + l_i) \\ \sin\theta_i & 0 & -\cos\theta_i & OB_{y_i} + \cos\theta_i (d_i + l_i) \\ 0 & 1 & 0 & 0 \\ 0 & 0 & 0 & 1 \end{bmatrix}
\end{aligned}
\tag{19}
$$

where i=1, 2, 3.

$$
\begin{aligned}
{}^{M_i}_{O_i}T^2 &= \begin{bmatrix} 1 & 0 & 0 & p_x \\ 0 & 1 & 0 & p_y \\ 0 & 0 & 1 & 0 \\ 0 & 0 & 0 & 1 \end{bmatrix} \begin{bmatrix} \cos(\lambda_i + \phi) & -\sin(\lambda_i + \phi) & 0 & 0 \\ \sin(\lambda_i + \phi) & \cos(\lambda_i + \phi) & 0 & 0 \\ 0 & 0 & 1 & 0 \\ 0 & 0 & 0 & 1 \end{bmatrix} \begin{bmatrix} 1 & 0 & 0 & PM_i \\ 0 & 1 & 0 & 0 \\ 0 & 0 & 1 & 0 \\ 0 & 0 & 0 & 1 \end{bmatrix} \\
&= \begin{bmatrix} \cos(\lambda_i + \phi) & -\sin(\lambda_i + \phi) & 0 & p_x + PM_i \cos(\lambda_i + \phi) \\ \sin(\lambda_i + \phi) & \cos(\lambda_i + \phi) & 0 & p_y + PM_i \sin(\lambda_i + \phi) \\ 0 & 0 & 1 & 0 \\ 0 & 0 & 0 & 1 \end{bmatrix}
\end{aligned}
\tag{20}
$$

where $\lambda_1 = \pi + \sigma_1$ and $\lambda_2 = -\sigma_2$. Since the position vectors of ${}^{M_i}_{O_i}T^1$ and ${}^{M_i}_{O_i}T^2$ matrices are equal, one can write easily the following equations.

$$
\begin{bmatrix} -\sin\theta_i (d_i + l_i) \\ \cos\theta_i (d_i + l_i) \end{bmatrix} = \begin{bmatrix} p_x + \upsilon_{x_i} \cos\phi - \upsilon_{y_i} \sin\phi - OB_{x_i} \\ p_y + \upsilon_{x_i} \sin\phi + \upsilon_{y_i} \cos\phi - OB_{y_i} \end{bmatrix} \tag{21}
$$

where $\upsilon_{x_i} = PM_i \cos\lambda_i$ and $\upsilon_{y_i} = PM_i \sin\lambda_i$. Summing the squares of the both sides in the equation 21, we obtain, after simplification,

$$
\begin{aligned}
Q_i = {} & p_x^2 + p_y^2 + OB_{x_i}^2 + OB_{y_i}^2 + \upsilon_{x_i}^2 + \upsilon_{y_i}^2 - 2p_x OB_{x_i} - 2p_y OB_{y_i} \\
& + 2\cos\phi (p_x \upsilon_{x_i} + p_y \upsilon_{y_i} - OB_{x_i} \upsilon_{x_i} - OB_{y_i} \upsilon_{y_i}) \\
& + 2\sin\phi (p_y \upsilon_{x_i} - p_x \upsilon_{y_i} - OB_{y_i} \upsilon_{x_i} + OB_{x_i} \upsilon_{y_i}) - (d_i + l_i)^2 = 0
\end{aligned}
\tag{22}
$$

The inverse kinematics problem is solved using the equation 22 as follows.

$$d_i = \sqrt{\begin{aligned} & p_x^2 + p_y^2 + OB_{x_i}^2 + OB_{y_i}^2 + \upsilon_{x_i}^2 + \upsilon_{y_i}^2 - 2p_x OB_{x_i} - 2p_y OB_{y_i} \\ & + 2\cos\phi(p_x\upsilon_{x_i} + p_y\upsilon_{y_i} - OB_{x_i}\upsilon_{x_i} - OB_{y_i}\upsilon_{y_i}) \\ & + 2\sin\phi(p_y\upsilon_{x_i} - p_x\upsilon_{y_i} - OB_{y_i}\upsilon_{x_i} + OB_{x_i}\upsilon_{y_i}) \end{aligned}} - l_i \qquad (23)$$

Once the d_1, d_2 and d_3 are obtained, the angles θ_1, θ_2 and θ_3 can be determined from the equation 21 by back substitution.

$$\theta_i = a\tan 2\left(-\frac{p_x + \upsilon_{x_i}\cos\phi - \upsilon_{y_i}\sin\phi - OB_{x_i}}{(d_i + l_i)}, \frac{p_y + \upsilon_{x_i}\sin\phi + \upsilon_{y_i}\cos\phi - OB_{y_i}}{(d_i + l_i)}\right) \qquad (24)$$

The forward kinematics problem is found rearranging the equation 22 as follows.

$$p_x^2 + p_y^2 + a_i p_x + b_i p_y + c_i = 0 \qquad (i=1,2,3) \qquad (25)$$

where $a_i = 2(\cos\phi\upsilon_{x_i} - OB_{x_i} - \sin\phi\upsilon_{y_i})$, $b_i = 2(\cos\phi\upsilon_{y_i} + \sin\phi\upsilon_{x_i} - OB_{y_i})$ and $c_i = OB_{x_i}^2 + OB_{y_i}^2 + \upsilon_{x_i}^2 + \upsilon_{y_i}^2 - 2\cos\phi(OB_{x_i}\upsilon_{x_i} + OB_{y_i}\upsilon_{y_i}) + 2\sin\phi(OB_{x_i}\upsilon_{y_i} - OB_{y_i}\upsilon_{x_i}) - (d_i + l_i)^2$

One can obtain the following new system of equations using equation 25.

$$\begin{aligned} (a_1 - a_2)p_x + (b_1 - b_2)p_y + (c_1 - c_2) &= 0 \\ (a_1 - a_3)p_x + (b_1 - b_3)p_y + (c_1 - c_3) &= 0 \\ (a_2 - a_3)p_x + (b_2 - b_3)p_y + (c_2 - c_3) &= 0 \end{aligned} \qquad (26)$$

One can write the following equations using the equation 26.

$$\begin{aligned} a_{12}p_x + b_{12}p_y &= c_{12} \\ a_{13}p_x + b_{13}p_y &= c_{13} \end{aligned} \qquad (27)$$

where $a_{12} = a_1 - a_2$, $b_{12} = b_1 - b_2$, $c_{12} = c_2 - c_1$, $a_{13} = a_1 - a_3$, $b_{13} = b_1 - b_3$ and $c_{13} = c_3 - c_1$. The p_x and p_y can be obtained applying the elimination method to the equation 27 as

$$p_x = \frac{b_{12}c_{13} - b_{13}c_{12}}{(b_{12}a_{13} - b_{13}a_{12})} \quad \text{and} \quad p_y = \frac{a_{13}c_{12} - a_{12}c_{13}}{(a_{13}b_{12} - a_{12}b_{13})} \qquad (28)$$

The orientation angle (ϕ) can be found using i=3 in equation 25.

$$p_x^2 + p_y^2 + a_3 p_x + b_3 p_y + c_3 = 0 \tag{29}$$

If p_x and p_y in equation 28 are substituted in equation 29, one can obtain after simplification

$$\chi^2 + \xi^2 + a_3 \chi \vartheta + b_3 \xi \vartheta + c_3 \vartheta^2 = 0 \tag{30}$$

where $\vartheta = (b_{12}a_{13} - b_{13}a_{12})$, $\chi = b_{12}c_{13} - b_{13}c_{12}$ and $\xi = a_{13}c_{12} - a_{12}c_{13}$. The equation 30 can be converted into the eight-degree polynomial using $\sin\phi = \frac{2t}{1+t^2}$ and $\cos\phi = \frac{1-t^2}{1+t^2}$. The roots of this polynomial are the answer of the forward kinematics problem. Once ϕ is determined, p_x and p_y can be found easily substituting the angle ϕ in equation 28. After having position (p_x, p_y) and orientation (ϕ), the passive joint angles can be found using the equation 21 by back substitution

$$\theta_i = A\tan 2\left(-\frac{p_x + \upsilon_{x_i}\cos\phi - \upsilon_{y_i}\sin\phi - OB_{x_i}}{(d_i + l_i)}, \frac{p_y + \upsilon_{x_i}\sin\phi + \upsilon_{y_i}\cos\phi - OB_{y_i}}{(d_i + l_i)} \right) \tag{31}$$

The Jacobian matrix of the 3-dof PPM shown in Figure 3 is computed as follows.

$$\begin{bmatrix} \frac{\partial Q_1}{\partial p_x} & \frac{\partial Q_1}{\partial p_y} & \frac{\partial Q_1}{\partial \phi} \\ \frac{\partial Q_2}{\partial p_x} & \frac{\partial Q_2}{\partial p_y} & \frac{\partial Q_2}{\partial p\phi} \\ \frac{\partial Q_3}{\partial p_x} & \frac{\partial Q_3}{\partial p_y} & \frac{\partial Q_3}{\partial p\phi} \end{bmatrix} \begin{bmatrix} \dot{p}_x \\ \dot{p}_y \\ \dot{\phi} \end{bmatrix} + \begin{bmatrix} \frac{\partial Q_1}{\partial d_1} & \frac{\partial Q_1}{\partial d_2} & \frac{\partial Q_1}{\partial d_3} \\ \frac{\partial Q_2}{\partial d_1} & \frac{\partial Q_2}{\partial d_2} & \frac{\partial Q_2}{\partial d_3} \\ \frac{\partial Q_3}{\partial d_1} & \frac{\partial Q_3}{\partial d_2} & \frac{\partial Q_3}{\partial d_3} \end{bmatrix} \begin{bmatrix} \dot{d}_1 \\ \dot{d}_2 \\ \dot{d}_3 \end{bmatrix} = 0$$

$$\begin{bmatrix} \delta_1 & \gamma_1 & \rho_1 \\ \delta_2 & \gamma_2 & \rho_2 \\ \delta_3 & \gamma_3 & \rho_3 \end{bmatrix} \begin{bmatrix} \dot{p}_x \\ \dot{p}_y \\ \dot{\phi} \end{bmatrix} + \begin{bmatrix} -d_1 - l_1 & 0 & 0 \\ 0 & -d_2 - l_2 & 0 \\ 0 & 0 & -d_3 - l_3 \end{bmatrix} \begin{bmatrix} \dot{d}_1 \\ \dot{d}_2 \\ \dot{d}_3 \end{bmatrix} = 0 \tag{32}$$

where

$$\delta_i = p_x - OB_{x_i} + \cos\phi\,\upsilon_{x_i} - \sin\phi\,\upsilon_{y_i} \tag{33}$$

$$\gamma_i = p_y - OB_{y_i} + \cos\phi\,\upsilon_{y_i} + \sin\phi\,\upsilon_{x_i} \tag{34}$$

$$\begin{aligned} \rho_i = &-\sin\phi(p_x\upsilon_{x_i} + p_y\upsilon_{y_i} - OB_{x_i}\upsilon_{x_i} - OB_{y_i}\upsilon_{y_i}) \\ &+ \cos\phi(p_y\upsilon_{x_i} - p_x\upsilon_{y_i} - OB_{y_i}\upsilon_{x_i} + OB_{x_i}\upsilon_{y_i}) \end{aligned} \tag{35}$$

The overall Jacobian matrix is obtained as

$$J = \begin{bmatrix} \frac{\delta_1}{d_1 + l_1} & \frac{\gamma_1}{d_1 + l_1} & \frac{\rho_1}{d_1 + l_1} \\ \frac{\delta_2}{d_2 + l_2} & \frac{\gamma_2}{d_2 + l_2} & \frac{\rho_2}{d_2 + l_2} \\ \frac{\delta_3}{d_3 + l_3} & \frac{\gamma_3}{d_3 + l_3} & \frac{\rho_3}{d_3 + l_3} \end{bmatrix} \tag{36}$$

***Numerical example for the inverse kinematics*:** The dimensions of the planar 3-dof RPR parallel manipulator are given as l_1=10, l_2=10, l_3=10, OB_{x1}=0, OB_{y1}=0, OB_{x2}=20, OB_{y2}=0, OB_{x3}=10, OB_{y3}=45, M_1M_2=15. The position of the point P in terms of the coordinate frame {xyz} attached to the M_1 corner of the moving platform is chosen as (4, 5). The angles λ_1, λ_2 and λ_3 are computed as 231.3402, -24.4440 and 66.3453, where $\sigma_1 = 51.3402$ and $\sigma_2 = 24.4440$, respectively. Moreover, the lengths PM_1, PM_2 and PM3 are determined as 6.4031, 12.0830 and 8.7233, respectively. If the position and orientation in terms of the base frame {XYZ} are given as p_x=12, p_y=18 and ϕ=30°, the active joint variables d_1 d_2 and d_3 can be found as 6.0617, 9.5881 and 8.3594, respectively. The passive joint variables θ_1, θ_2 and θ_3 are found as -43.4006, -11.8615 and -176.7655, respectively by back substitution.

Numerical example for the forward kinematics: The dimensions of manipulator are given as l_1=11, l_2=11, l_3=11, OB_{x1}=0, OB_{y1}=0, OB_{x2}=10, OB_{y2}=0, OB_{x3}=5, OB_{y3}=32, M_1M_2=10. The position of the point P in terms of the coordinate frame {xyz} is chosen as (5, 2.8868). The angles λ_1, λ_2 and λ_3 are computed as 210.0004, -30.0004 and 90, where $\sigma_1 = 30$ and $\sigma_2 = 30.0004$, respectively. Moreover, the lengths PM_1, PM_2 and PM_3 are determined as 8.4853, 7.8102 and 3.5616, respectively. If the active and passive joint variables are given as d_1=8, d_2=7.9999, d_3=7.9999 and θ_1=-52.1046, θ_2=-52.105, θ_3=-127.8937, the position and orientation of end-effector in terms of base coordinate frame {XYZ} are found as p_x=19,9936 p_y=14.5569 and ϕ=0.000932°, respectively.

Numerical example for the Jacobian matrix and condition number: Using the dimensions of numerical example for the inverse kinematics above, the Jacobian matrix and condition number are found as

$$J = \begin{bmatrix} 0.6871 & 0.7266 & 3.6489 \\ 0.2055 & 0.9786 & 11.5290 \\ 0.0564 & -0.9984 & 0.4734 \end{bmatrix} \text{ and } \kappa = 8.1351 \tag{37}$$

Numerical example for the workspace determination: The dimensions of the manipulator are given as l_1=l_2=l_3=8.5, OB_{x1}=0, OB_{y1}=0, OB_{x2}=17, OB_{y2}=0, OB_{x3}=9, OB_{y3}=40, M_1M_2=16. The lengths of the actuated prismatic joints vary between d_i(min)=0 and d_i(max)=8.5, where i=1,2,3. If the position of the point P in terms of the coordinate frame {xyz} is chosen as (7, 7), the angles λ_1, λ_2 and λ_3 are computed as 225, -37.8750 and 81.7020, where $\sigma_1 = 45$ and

$\sigma_2 = 37.8750$, respectively. Moreover, the lengths PM_1, PM_2 and PM_3 are determined as 9.8995, 11.4018 and 6.9289, respectively. The workspace is obtained as 110.6180 for ϕ=0° orientation. The red rectangle given by Figure 4 illustrates the limits of the discretized Cartesian area. Additionally, the black region shows the reachable workspaces of the manipulator.

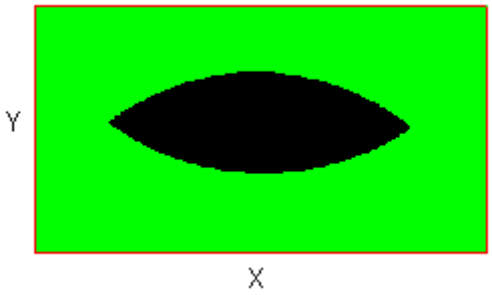

Fig. 4. The workspace of the planar 3-dof RPR parallel manipulator.

Numerical example for the dexterity and singularity analysis: The Figure 5 shows the inverse dexterity of the manipulator using the same dimensions given by the example for workspace determination. The GDI of the manipulator is found as 0.00018179. As can be illustrated in Figure 5, as the inverse of the condition numbers increase the manipulator accomplish better gross motion capability like the regions represented with red color. At the same time, the diagonal line divides the workspaces of the manipulator into two regions, illustrates the singular points. The dark blue areas illustrate the non-reachable workspaces of the manipulator.

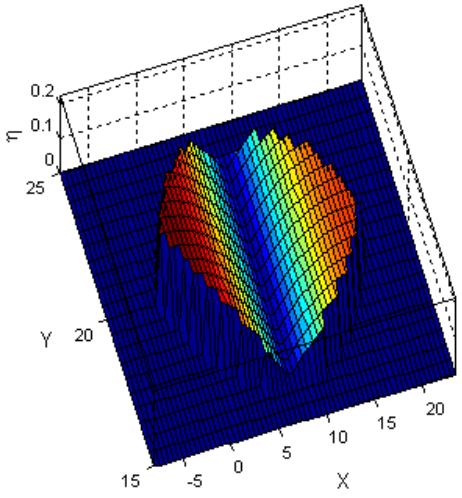

Fig. 5. The inverse dexterity graph for planar 3-dof RPR parallel manipulator.

4. Conclusion

In this book chapter, the forward and inverse kinematics problems of planar parallel manipulators are obtained using Denavit & Hartenberg (1955) kinematic modelling convention. Afterwards some fundamental definitions about Jacobian matrix, condition number, global dexterity index, singularity and workspace determination are provided for performing the analyses of a two-degree-of-freedom (2-dof) PPM and a 3-dof Fully Planar Parallel Manipulator.

5. References

Agrawal, S. K. (1990). Workspace boundaries in-parallel manipulator systems. *Int. J. Robotics Automat*, Vol., 6(3), pp. 281-290

Bonev, I. A. & Ryu, J. (2001). A geometrical method for computing the constant-orientation workspace of 6-PRRS parallel manipulators. *Mechanism and Machine Theory*, Vol., 36 (1), pp. 1–13

Denavit, J. & Hartenberg, R. S., (1955). A kinematic notation for lower-pair mechanisms based on matrices. *Journal of Applied Mechanics*, Vol., 22, 1955, pp. 215–221

Fichter, E. F. (1986). A Stewart platform-based manipulator: General theory and practical consideration. *Journal of Robotics Research*, pp. 157-182

Gosselin C., (1990). Determination of the workspace of 6-d.o.f parallel manipulators. *ASME Journal of Mechanical Design*, Vol., 112, 1990, pp. 331-336

Gosselin, C. & Angeles, J. (1991). A global performance index for the kinematic optimization of robotic manipulators. *Journal of Mech Design*, Vol., 113, 1991, pp. 220-226

Gosselin, C. M. & Guillot, M. (1991). The synthesis of manipulators with prescribed workspace. *Journal of Mechanical Design*, Vol., 113, pp. 451–455

Heerah, I.; Benhabib, B.; Kang, B. & Mills, K. J. (2003). Architecture selection and singularity analysis of a three-degree-of freedom planar parallel manipulator. *Journal of Intelligent and Robotic Systems*, Vol., 37, 2003, pp. 355-374

Hubbard, T.; Kujath, M. R. & Fetting, H. (2001). MicroJoints, Actuators, Grippers, and Mechanisms, *CCToMM Symposium on Mechanisms, Machines and Mechatronics,* Montreal, Canada

Kang, B.; Chu, J. & Mills, J. K. (2001). Design of high speed planar parallel manipulator and multiple simultaneous specification control, *Proceedings of IEEE International Conference on Robotics and Automation*, pp. 2723-2728, South Korea

Kang, B. & Mills, J. K. (2001). Dynamic modeling and vibration control of high speed planar parallel manipulator, *In Proceedings of IEEE/RJS International Conference on Intelligent Robots and Systems,* pp. 1287-1292, Hawaii

Kim, D. I.; Chung, W. K. & Youm, Y. (1997). Geometrical approach for the workspace of 6-DOF parallel manipulators, *Proceedings of IEEE International Conference on Robotics and Automation*, pp. 2986-2991, Albuquerque, New Mexico

Merlet, J. P. (1995). Determination of the orientation workspace of parallel manipulators. *Journal of Intelligent and Robotic Systems*, Vol., 13, pp. 143-160

Merlet, J. P. (1996). Direct kinematics of planar parallel manipulators, *Proceedings of IEEE International Conference on Robotics and Automation*, Vol., 4, pp. 3744-3749

Merlet, J. P.; Gosselin, C. M. & Mouly, N. (1998). Workspaces of planar parallel manipulators. *Mechanism and Machine Theory*, Vol., 33, pp. 7–20

Merlet, J. P. (2000). *Parallel robots*, Kluwer Academic Publishers

Tsai, L. W. (1999). *Robot analysis: The mechanics of serial and parallel manipulators*, A Wiley-Interscience Publication

Robot Manipulators New Achievements

Edited by Aleksandar Lazinica and Hiroyuki Kawai

ISBN 978-953-307-090-2
Hard cover, 718 pages
Publisher InTech
Published online 01, April, 2010
Published in print edition April, 2010

Robot manipulators are developing more in the direction of industrial robots than of human workers. Recently, the applications of robot manipulators are spreading their focus, for example Da Vinci as a medical robot, ASIMO as a humanoid robot and so on. There are many research topics within the field of robot manipulators, e.g. motion planning, cooperation with a human, and fusion with external sensors like vision, haptic and force, etc. Moreover, these include both technical problems in the industry and theoretical problems in the academic fields. This book is a collection of papers presenting the latest research issues from around the world.

How to reference

In order to correctly reference this scholarly work, feel free to copy and paste the following:

Serdar Kucuk (2010). Kinematics, Singularity and Dexterity Analysis of Planar Parallel Manipulators Based on DH Method, Robot Manipulators New Achievements, Aleksandar Lazinica and Hiroyuki Kawai (Ed.), ISBN: 978-953-307-090-2, InTech, Available from: http://www.intechopen.com/books/robot-manipulators-new-achievements/kinematics-singularity-and-dexterity-analysis-of-planar-parallel-manipulators-based-on-dh-method

INTECH
open science | open minds

InTech Europe
University Campus STeP Ri
Slavka Krautzeka 83/A
51000 Rijeka, Croatia
Phone: +385 (51) 770 447
Fax: +385 (51) 686 166
www.intechopen.com

InTech China
Unit 405, Office Block, Hotel Equatorial Shanghai
No.65, Yan An Road (West), Shanghai, 200040, China
中国上海市延安西路65号上海国际贵都大饭店办公楼405单元
Phone: +86-21-62489820
Fax: +86-21-62489821